Available online at www.sciencedirect.com
ScienceDirect
Surface Science 601 (2007) 2896–2907
SURFACE SCIENCE
www.elsevier.com/locate/susc

High-resolution photoemission studies of the interfacial reactivity and interfacial energetics of Au and Cu Schottky barriers on methyl-terminated Si(1 1 1) surfaces

Ralf Hunger [a,*], Rainer Fritsche [a], Bengt Jaeckel [a], Lauren J. Webb [b], Wolfram Jaegermann [a], Nathan S. Lewis [b]

[a] *Institute of Materials Science, Technische Universität Darmstadt, Petersenstr. 23, 64287 Darmstadt, Germany*
[b] *Division of Chemistry and Chemical Engineering, Beckman Institute and Kavli Nanoscience Institute, California Institute of Technology, 210 Noyes Laboratory, 127-72, Pasadena, CA 91125, USA*

Received 12 October 2006; accepted for publication 23 April 2007
Available online 8 May 2007

Abstract

The Schottky junction formation by the stepwise evaporation of gold and copper, respectively, onto methyl-terminated silicon, CH_3–Si(1 1 1), was investigated by synchrotron X-ray photoelectron spectroscopy. During the junction formation process, interface reactions occurred as revealed by the appearance of chemically shifted Si 2p components. Upon deposition of Au, the formation of about one monolayer of gold silicide, $SiAu_3$, with a Si 2p chemical shift of +0.75(2) eV, was observed. The $SiAu_3$ floated on top of the growing gold layer. Similarly, for the deposition of Cu, the methyl termination layer was partially disrupted, as indicated by the appearance of a −0.28(2) eV chemically shifted Si 2p component attributable to an interfacial copper silicide phase, $SiCu_3$. Hence, the termination of the Si(1 1 1) surface by methyl groups did not completely prevent interfacial reactions, but did reduce the amount interfacial reaction products as compared to bare Si(1 1 1)-(7 × 7) surfaces.

Electron Schottky barrier heights of 0.78(8) eV (Au) and 0.61(8) eV (Cu) were measured. Within the experimental uncertainty the observed Schottky barriers were identical to those ones obtained on non-passivated, (7 × 7)-reconstructed Si(1 1 1) surfaces. Thus, the modification of the electronic properties of the silicon–metal contact requires the complete absence of interfacial reactions.
© 2007 Elsevier B.V. All rights reserved.

Keywords: Synchrotron radiation photoelectron spectroscopy; Silicon; Copper; Gold; Metal–semiconductor interfaces; Schottky barrier; Alkanes; Silicides

1. Introduction

Alkylation of Si(1 1 1) surfaces has been widely explored for its ability to impart molecular level control over the chemical and electrical properties of Si surfaces. Alkyl groups have been introduced through direct Si–C bonds using UV or thermally catalyzed olefin addition [1–4], electrochemical polarization, or reaction of the Cl-terminated Si surface with organic Grignard or Li reagents [5–12], amongst other methods. Methyl groups are the only saturated alkyl group that sterically can terminate every Si atop site on an unreconstructed Si(1 1 1) surface [13], hence CH_3–Si(1 1 1) surfaces are especially interesting. The CH_3–Si(1 1 1) surface, as well as other alkylated Si surfaces, can be prepared by a two-step chlorination/alkylation method [5,14]. Alklyation has been shown to improve the resistance to chemical and electrochemical oxidation of Si relative to the H-terminated Si(1 1 1) surface [6,8,14,15], to provide a low density of electrically active surface states [11,12,14,15], and to modify the surface dipole relative to that at H–Si(1 1 1) surfaces [12].

* Corresponding author. Tel.: +49 30 6392 5699; fax: +49 30 6392 5752.
E-mail addresses: hunger@surface.tu-darmstadt.de (R. Hunger), jaegerw@surface.tu-darmstadt.de (W. Jaegermann), nslewis@caltech.edu (N.S. Lewis).

0039-6028/$ - see front matter © 2007 Elsevier B.V. All rights reserved.
doi:10.1016/j.susc.2007.04.249

Fermi-level pinning and metal silicide formation are both commonly observed on Si(1 1 1)–metal Schottky barriers. A question of interest is the extent to which modification of the Si surface with a $–CH_3$ group can effect a modification in the electrical and chemical properties of such Si–metal Schottky barriers. Hence, in this work, we report studies of the energetics and interfacial chemistry of CH_3–Si(1 1 1) surfaces onto which Schottky barrier contacts have been formed with Au and Cu. Au and Cu have different work functions but are well-known to be reactive with Si [16–24]. Studies of these contacts therefore ought to provide information on whether Fermi-level pinning can be controlled by introduction of $–CH_3$ groups onto the Si surface. The reactivity and energetics of the interfaces have been probed using high-resolution synchrotron photoemission methods, which provides information on the chemical state of the interface as well as on the electrical properties, including the band bending, interfacial dipole, and barrier heights, of the Si–metal contacts of interest.

2. Experimental

2.1. Materials and methods

2.1.1. Materials

Silicon(1 1 1) wafers polished on one side to a thickness of 380 μm with a miscut angle of ±0.5° were obtained from ITME (Poland). These n-type samples were doped with Sb to a resistivity of 0.005–0.02 Ω cm. This doping level corresponds to a Fermi level position in the bulk of the wafers of 1.04(2) eV above the valence band maximum, E_v.

All solvents used in alkylation reactions were anhydrous, stored under N_2(g), and used as received from Aldrich Chemical Corp. Solvents were only exposed to the atmosphere of a N_2(g)-purged flush box. Water with a resistivity >18.0 MΩ cm was used at all times. All other chemicals were used as received.

2.1.2. Sample preparation

Before chemical functionalization, each sample was cleaned by rinsing in a flowing stream of H_2O, CH_3OH, acetone, CH_3OH, and H_2O, respectively. After cleaning, the sample was placed directly in 11 M (i.e., 40% by weight) NH_4F(aq) (Transene, Inc.) for 20 min to etch the native oxide layer and produce a H-terminated Si(1 1 1) surface. During the etching process, the wafers were agitated occasionally to remove the bubbles that formed on the surface. After removal from the etching solution, the sample was rinsed thoroughly with H_2O and dried under a stream of N_2(g). The sample was then placed into the antechamber of a N_2(g)-purged glove-box for further chemical functionalization.

Hydrogen-terminated Si(1 1 1) surfaces were chlorinated according to previously published procedures. A freshly etched surface was first immersed in a saturated solution of PCl_5 (99.998%, Alfa Aesar) in chlorobenzene to which a few grains of benzoyl peroxide had been added. The reaction solution was then heated to 90–100 °C for 45 min. The sample was then removed from the reaction solution, rinsed with tetrahydrofuran (THF) and CH_3OH, and dried with a stream of N_2(g).

For alkylation, the Cl-terminated Si(1 1 1) sample was immersed in a 3 M solution of CH_3MgBr in THF (Aldrich). Excess THF was added to each reaction solution to allow for solvent loss. The reaction solution was heated to 70–80 °C for 5 h. At the end of the reaction, the sample was removed from the solution and rinsed with copious amounts of THF and CH_3OH, then immersed in CH_3OH and removed from the N_2-purged glove-box. The sample was sonicated for 5 min in CH_3OH, sonicated in CH_3CN for a further 5 min, and then dried under a stream of N_2(g). Sonication was required for complete removal of adsorbed Mg salts from the surface of the sample. The CH_3-terminated Si(1 1 1) samples were then sealed under N_2(g) and transported to the BESSY synchrotron facility in Berlin. Samples were received in <2 days from the time of preparation, and then stored in an Ar-purged glove-box with H_2O and O_2 concentrations of ⩽ 1 ppm for 10 further days.[1] The samples were then mounted onto OMICRON®-type sample holders and introduced into the vacuum system.

2.2. Metal deposition

Gold and copper were deposited by physical vapor deposition in an ultra-high vacuum deposition chamber that was equipped with direct vacuum transfer to the analysis system [25]. Gold was deposited using a water-cooled effusion cell, whereas Cu was evaporated using a home-made Knudsen cell. Prior to the metal deposition the samples were vacuum annealed for 20 min at ≈390 °C to desorb any adventitious, weakly bound non-methyl hydrocarbon contamination [12]. During depositions, the CH_3–Si(1 1 1) substrates were not heated and were thus nominally at room temperature (not accounting for adventitious heating of the sample due to heat radiated from the hot crucibles during deposition). The deposition experiments were conducted at cell temperatures of 1250 °C for Au and 1130 °C for Cu. The deposition rate of copper was 2.8 Å min^{-1}, as measured prior to the experiments by a quartz crystal flux monitor. The deposition rate of gold was estimated as 0.57 Å min^{-1} by measurement of the attenuation of the Si 2p signal produced by the first, submonolayer, deposition steps. The thickness of a monolayer (ML) of deposited material was 2.6 Å (Au) or 2.3 Å (Cu), as calculated from the bulk parameters for the metal

[1] During glove-box storage for up to 2 weeks, no significant deterioration of the methylated silicon surface was observed in terms of oxidation or hydrocarbon contamination. The excellent chemical stability of Si(1 1 1)–CH_3 is also evidenced by the substantial inhibition of oxidation in ambient air in comparison to the hydrogen-passivated Si(1 1 1)–H surface (Ref. [14]).

Table 1
Deposition steps of Au on CH_3–Si(1 1 1)

Cumulative deposition time (s)	Nominal Au thickness (Å)	Nominal thickness (ML)
0	0	0
5	0.06	0.02
10	0.11	0.04
20	0.22	0.09
50	0.56	0.21
125	1.4	0.54
300	3.4	1.3
480	5.4	2.1
960	11	4.1
1440	16	6.2
1920	21	8.2
4800	54	21

The thickness of a monolayer of Au corresponds to 2.6 Å [26].

Table 2
Deposition steps of Cu on CH_3–Si(1 1 1)

Cumulative deposition time (min)	Nominal Cu thickness (Å)	Nominal Cu thickness (ML)
0	0	0
0.17	0.5	0.21
0.5	1.4	0.61
1.5	4.2	1.8
4.5	13	5.5
13.5	38	16
26	73	32
90	252	110

The thickness of a monolayer (ML) of Cu corresponds to 2.3 Å [26].

of interest [26].[2] Tables 1 and 2 present the deposition steps, the respective accumulated deposition time, and the corresponding calculated coverage of metal, for each experiment. For each metal, a complete deposition run was performed up to a deposited thickness at which the substrate Si^0 emission was no longer detectable. To ascertain whether the substrate vacuum annealing to ~390 °C before the metal deposition affected the interfacial reactivity, gold was also deposited in a single evaporation step of 1440 s onto a non-annealed, as received CH_3–Si(1 1 1) substrate. The result was identical to the deposition on the annealed CH_3–Si(1 1 1) surface.

2.3. SXPS analysis and data processing

Before and after every metal deposition step, the silicon surfaces were characterized by synchrotron-excited soft X-ray photoelectron spectroscopy (SXPS). The experiments were conducted in the SoLiAS experimental station [25] on the U49/2-PGM2 undulator beamline of the synchrotron storage ring BESSY II. High-resolution photoelectron spectra were recorded in normal emission with a Phoibos 150-MCD9 analyzer (SPECS) using photon excitation energies, E_{ex}, of 1253 eV (Cu $2p_{3/2}$), 330 eV, 240 eV, and 150 eV. The combined experimental resolution (photon and electron analyzer broadening) was 85 meV ($h\nu = 150$ eV) and 115 meV ($h\nu = 240$ eV), respectively, as determined from the broadening of the Fermi edge of freshly deposited metal films. In addition, using a He gas discharge lamp, ultraviolet photoelectron spectra of the valence band region were collected using $E_{ex} = 21.22$ eV.

The core level spectra were decomposed into symmetrical, Gaussian–Lorentzian broadened Voigt profiles using curve fitting routines implemented in Wavemetrics' Igor Pro 4.09. For the Si 2p core level, the spin–orbit splitting was set to 0.607 eV and the ratio of the Si $2p_{1/2}$ to Si $2p_{3/2}$ peak areas was set to 0.51 [12]. The Lorentzian widths were fixed at 0.05 eV (Si 2p [12]), 0.14 eV (Au 4f), and 0.15 eV (C 1s), respectively [12]. The peak positions, intensities, and Gaussian widths were allowed to vary and were adjusted to best fit the measured data.

3. Results

3.1. Interface formation with Au

3.1.1. Si 2p spectra at E_{ex} = 240 and 150 eV

Fig. 1 shows the Si 2p and Au $4f_{7/2}$ core level photoemission spectra with $E_{ex} = 240$ eV for the stepwise deposition of Au on CH_3–Si(1 1 1). Consistent with previous studies [10,12,27], two pairs of spin–orbit doublets, one ascribed to bulk Si, and the other ascribed to Si bonded to the more electronegative C, were observed in the Si 2p region of the native CH_3–Si(1 1 1) surface.

As metal was deposited, the Si 2p emission shifted to lower binding energy, indicative of a change in band bending in the Si as the metal overlayer was formed. Additionally, the Si 2p emission intensity decreased with increasing amounts of metal deposition. For Au film thicknesses $\geqslant$ 0.5 ML, a third component of the Si 2p signal was observed, with a chemical shift of +0.75(2) eV with respect to the bulk Si^0 emission. This signal increased in intensity as the cumulative Au film thickness increased from 0.5 to 8 ML, and then remained constant as the Au coverage increased from 8 ML to 21 ML.

Fig. 2 depicts the Si 2p spectra obtained using the most surface-sensitive excitation energy, $E_{ex} = 150$ eV. At this excitation energy, the Si 2p signals derived from surface and bulk Si atoms exhibit approximately equal intensities [12]. Fig. 2 also displays the components of the observed Si 2p signal deduced by curve fitting of the SXPS data. For cumulative Au film thickness $\geqslant$0.5 ML, the generation and intensity increase of a third Si 2p component, shifted by +0.75(2) eV from the Si^0 bulk emission, is clearly evident. After the last, large deposition step of Au (involving the deposition of 13 ML of additional film thickness), the substrate Si^0 2p signal was no longer detectable. The high

[2] This definition should not be confused with another often used convention for a monolayer, namely, of the number density of atoms corresponding to 7.8×10^{-14} cm^2, the surface site density of Si(1 1 1). Using this alternative definition and the bulk atom density of Cu or Au, monolayer thicknesses of 1.3 Å (Au) and 0.9 Å (Cu) are obtained, in contrast to the definition used in this work.

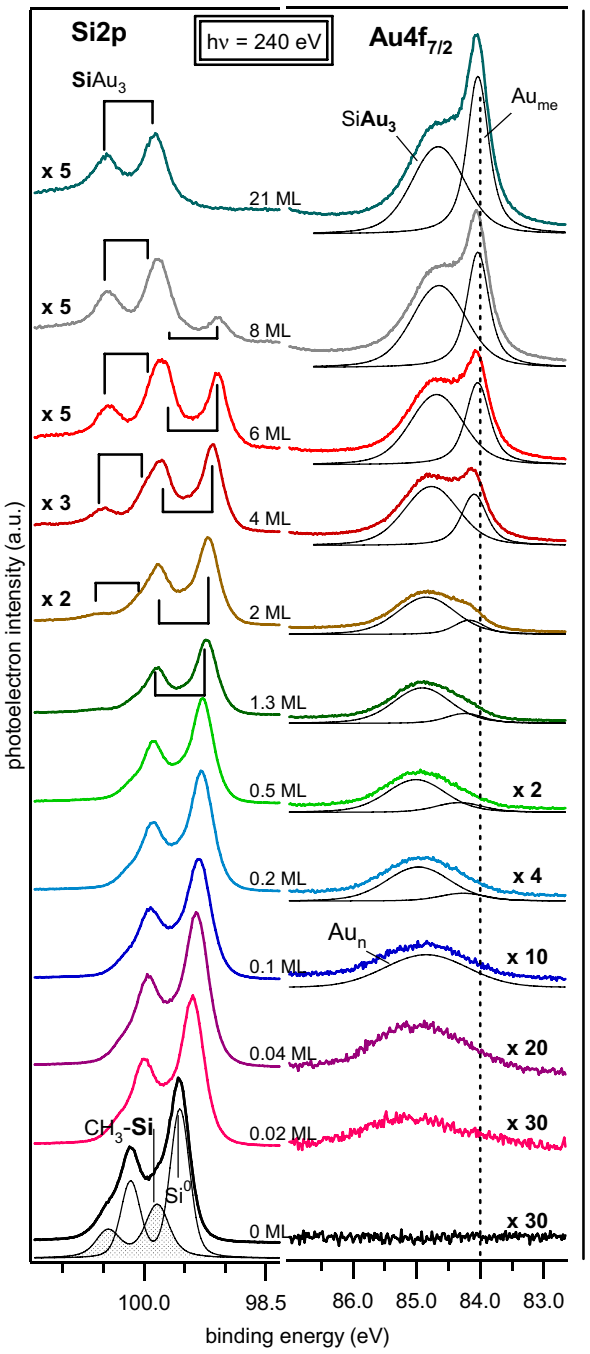

Fig. 1. Si 2p and Au $4f_{7/2}$ core levels excited with $E_{ex} = 240$ eV as a function of the cumulative deposition of Au onto the CH_3–Si(1 1 1) surface. The substrate Si 2p emission is an overlay of bulk (Si^0) and surface (CH_3–Si) contributions. The occurrence of a Si 2p signal ascribable to $SiAu_3$ is indicative of an interfacial reaction. The Au $4f_{7/2}$ region of the spectrum exhibits peaks for the $SiAu_3$ alloy, metallic, elemental Au (Au_{me}), and small, non-metallic Au clusters (Au_n). Some of the spectra were scaled and the scaling factors are indicated.

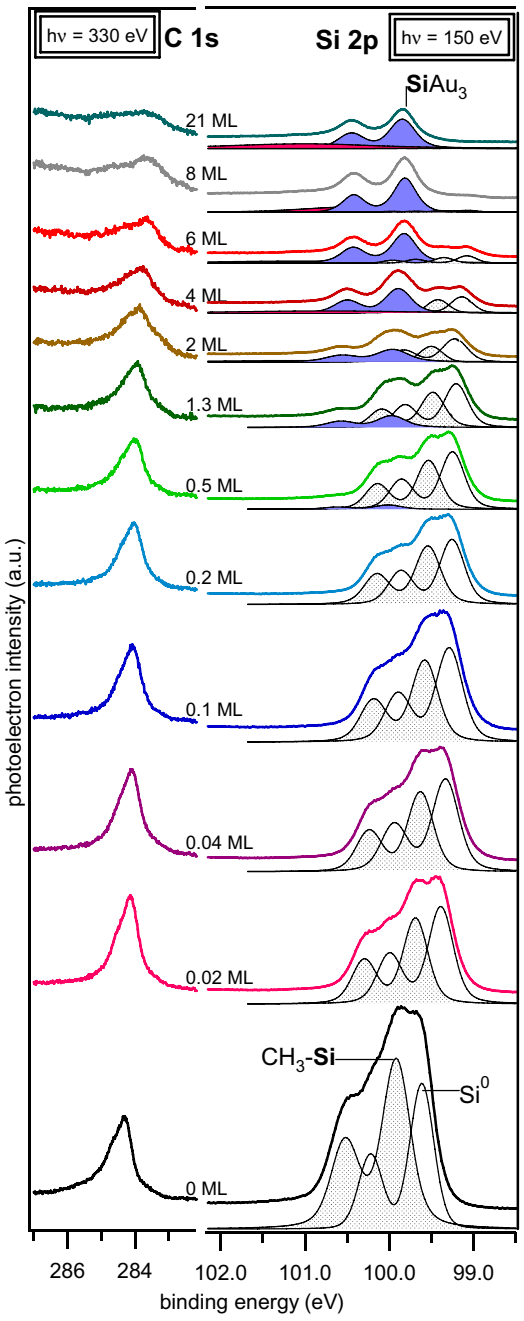

Fig. 2. C 1s core level ($E_{ex} = 330$ eV) and highly surface-sensitive Si 2p emission ($E_{ex} = 150$ eV) of the stepwise deposition of Au onto the CH_3–Si(1 1 1) surface. The shaded spectra are peak fits to the data, showing signals from bulk Si^0, from CH_3 bound surface Si atoms, and from the forming $SiAu_3$ alloy, respectively.

binding energy Si 2p signal has been ascribed to Au silicide, $SiAu_3$ [18,19]. For nominal Au film thickness >5 ML the intensity of this emission did not change significantly as further Au was deposited. This behavior indicates that the observed $SiAu_3$ was on top of the deposited Au film.

Fig. 3 displays plots of the intensities of the Si $2p_{3/2}$, Au $4f_{7/2}$, and C 1s emissions, from the data of Figs. 1 and 2, as a function of the nominal Au film thickness deposited onto the CH_3–Si(1 1 1) surface. For the last three deposition steps resulting in 6, 8, and 21 ML, respectively, of Au, the intensity of the $SiAu_3$ Si 2p emission remained essentially constant at 7.3×10^4 cps (with cps = counts per second), i.e., approximately 1/3 of the Si $2p^0_{3/2}$ emission intensity of 23×10^4 cps that was observed after the first

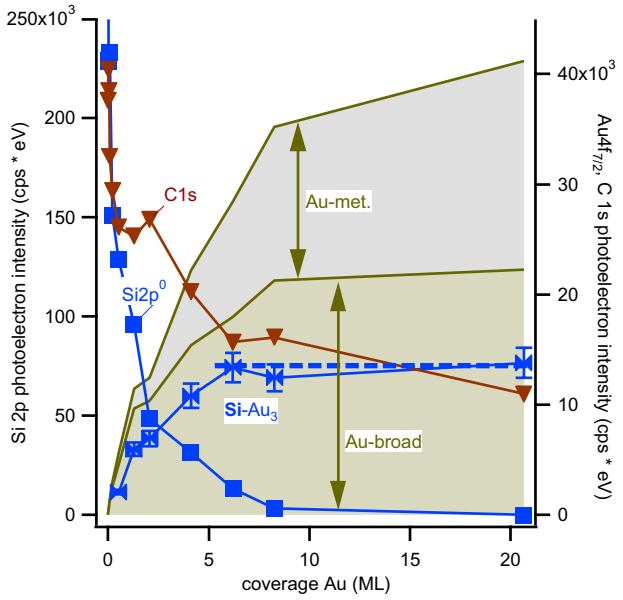

Fig. 3. Evolution of the Si 2p (with $E_{ex} = 150$ eV), Au $4f_{7/2}$ (with $E_{ex} = 240$ eV), and C 1s (with $E_{ex} = 330$ eV) SXPS signal intensities during the series of Au depositions. The persistence of the reacted $SiAu_3$ component indicates that the $SiAu_3$ layer is on top of the Au film. The narrow, metallic Au 4f component (Au-met.) at 84.0 eV is ascribable to metallic Au underneath the $SiAu_3$ region.

three deposition steps (0.02, 0.04, and 0.09 ML). Assuming that the intensity of the Si–CH_3 Si 2p emission corresponds to that of a silicon monolayer (surface atom density $N_{Si(111)} = 7.8 \times 10^{14}$ cm^{-2}) that was attenuated by the terminating methyl groups by a factor of $e^{-0.19/\lambda} \approx 0.75$ (Si–C bond length of 0.19 nm, escape depth $\lambda = 0.35$ nm [28]), the data indicate that the Si 2p[$SiAu_3$] emission intensity corresponds to transformation of 0.28 monolayers of silicon into $SiAu_3$. Hence, the amount of $SiAu_3$ formed is equivalent to ≈1 ML of $SiAu_3$, assuming that the atom densities of Si and $SiAu_3$ are comparable and that the film is laterally homogenous in structure.

3.1.2. Au 4f spectra at E_{ex} = 240 eV

Fig. 1b displays the SXPS data in the Au 4f region. At high Au coverage, the Au 4f emission consisted of a sharp, low binding energy component at 84.04(2) eV and of a broader, higher binding energy component that was shifted by +0.62(2) eV. These spectral components have been observed previously [18,19] for the Si(1 1 1)-7 × 7/Au interface. The broad, high binding energy component has been ascribed to emission from the surface layer of $SiAu_3$ and the sharp signal has been assigned to metallic Au [18,19].

The evolution of the metallic component was evident in the Au 4f SXPS data for nominal Au film thickness of 0.2 ML and more. Even at this low coverage of Au, a clear asymmetry of the Au 4f SXPS signal indicated the superposition of two components. At higher coverage, the (metallic) low binding energy Au 4f component sharpened (Gaussian width of 0.72 eV for 0.2 ML of Au to 0.22 eV for 21 ML of nominal Au film thickness) and shifted to lower binding energy (from 84.27(5) eV for 0.2 ML to 84.04(2) eV for 21 ML Au).[3]

A similar development of metallic character of the deposited Au film was observed in the valence band data obtained using ultraviolet photoemission spectroscopy (UPS) with $E_{ex} = 21.22$ eV (data not shown). Indications of step-like emission, close in energy to the Fermi energy characteristic of a metallic Au Fermi edge, were clearly evident in the UPS data for a nominal Au film thickness ⩾0.5 ML.

For all Au film thicknesses > 0.5 ML, the observation of spectral features characteristic of non-reacted, metal-like Au correlated with the appearance of, and subsequent increase in, the $SiAu_3$ silicide component in the Si 2p region of the SXPS data (cf. intensity plot in Fig. 3). The broad, high binding energy component of the Au 4f emission, however, was observable before the detectable onset of $SiAu_3$ formation in the Si 2p region of the SXPS spectra. This behavior indicates the presence of a third Au 4f component at low Au coverages, labeled Au_n, which can be ascribed to clusters of non-reacted Au.

3.1.3. C 1s spectra at E_{ex} = 330 eV

Fig. 2 also displays the C 1s emission measured using $E_{ex} = 330$ eV as a function of the amount of Au deposited onto CH_3–Si(1 1 1). The asymmetry of the C 1s emission of the clean CH_3–Si(1 1 1) surface has been ascribed to vibrational loss satellites arising from C–H stretch excitations on the high binding energy side of the peak [12]. During the deposition of Au, the C 1s signal intensity decreased and the line shape broadened, yielding evidence for new emissions on the low and high binding energy side of the main peak. Even for the highest Au coverage, the C 1s emission was observable at ≈37% of the intensity of the signal observed on the pristine CH_3–Si(1 1 1) monolayer. This behavior is consistent with the hypothesis that the carbonaceous fragments float on top of the Au/Au_3Si film surface.

In the first stage of Au deposition (up 0.5 ML), the intensity of the C 1s signal decreased at approximately the same rate as that observed for the Si 2p Si^0 and Si^{+1}–CH_3 emissions (Fig. 3). However, for longer deposition times and thus higher Au film thicknesses, the C 1s emission was less attenuated than the Si 2p substrate emissions. For the clean CH_3–Si(1 1 1) surface, the intensity ratio C 1s[330 eV]:Si 2p[Si^{+1}–CH_3, 150 eV] was 5.6, whereas for the thickest Au films (21 ML), the C 1s[330 eV]:Si 2p[$SiAu_3$, 150 eV] intensity ratio was 5.0. Hence, the ratio of the surface densities of carbon and silicon atoms was

[3] The photoelectron emission from metals is in principle asymmetric with a tail towards higher binding energies due to inelastic intra-band excitations. Such an asymmetric lineshape is usually fitted by Doniach–Sunjic functions. Even though this asymmetric broadening was neglected in our fitting approach, which used symmetric Voigt functions, the spectra nevertheless could be deconvoluted appropriately.

nearly identical for the clean surface and for the $SiAu_3$ surface layer, even for deposition of relatively thick layers of Au. This behavior suggests that the carbon-bonded silicon surface atoms disconnected from the silicon surface and became embedded into the $SiAu_3$ surface layer. Initially, the [Si–CH_3] units are therefore apparently incorporated into the surface silicide. The broadening of the C 1s emission, with new contributions on the high and low binding energy side of the signal as further Au was deposited, can be assigned to a SiC species (BE[C 1s] = 284.7(1) eV, cf. Fig. 7) and to the electron-stripped CH_{3-x} ($x > 0$) species at ~283.4 eV [29].

3.1.4. Si 2p binding energy vs coverage

Fig. 4 presents a plot of the binding energy of the bulk Si^0 Si $2p_{3/2}$ component as a function of the coverage of deposited Au. The figure includes the fitted data from the Si 2p spectra obtained using $E_{ex} = 330$, 240 and 150 eV. The binding energies clearly shifted in parallel, regardless of the excitation energy. The observed shift is therefore ascribable to the band bending induced by the deposition of metal.

Subtraction of the binding energy of the Si $2p_{3/2}$ emission with respect to the valence band maximum (VBM), BE_v(Si $2p_{3/2}$) = 98.74(4) eV [30], yielded the distance between the Fermi level, E_F, and the top of the valence band, E_v (right axis). For Au coverages of 6 ML and 8 ML, the value of $E_F - E_v$ remained constant at 0.34 eV above the VBM, indicating that the band bending induced by the Au overlayer had been completed. These data yielded an electronic Schottky barrier height for electrons, $\Phi_{B,n}$, of (1.12–0.34) eV = 0.78(8) eV for the n-type CH_3–Si(1 1 1)/Au Schottky contact.

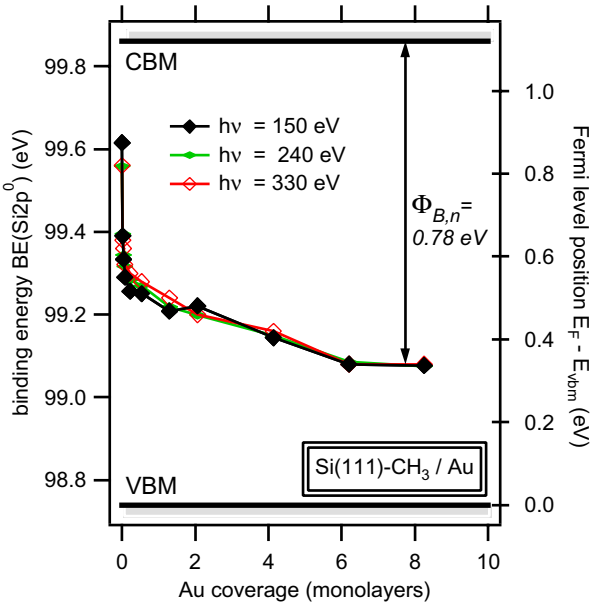

Fig. 4. Evolution of the band bending in the silicon as a function of the deposition of Au onto the CH_3–Si(1 1 1) surface, as monitored by the binding energy shift of the Si $2p_{3/2}$ emission. A Schottky barrier height of 0.78(8) eV is obtained using $BE_v(Si^0\ 2p) = 98.74(4)$ eV.

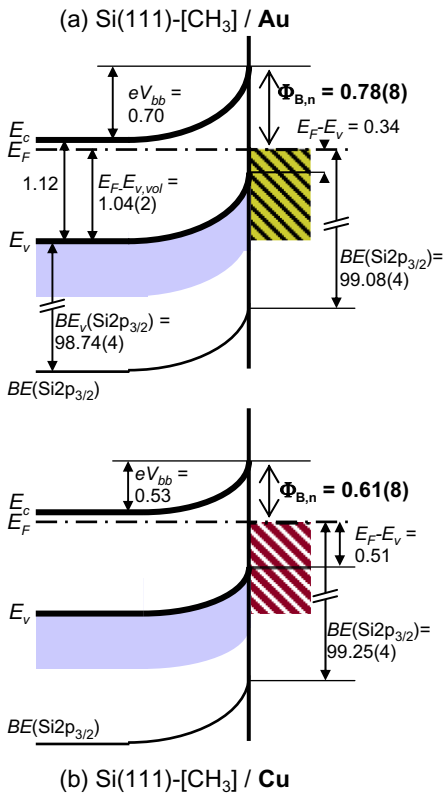

Fig. 5. Energy band diagrams of the CH_3–Si(1 1 1)/Au (top, a) and CH_3–Si(1 1 1)/Cu (bottom, b) Schottky contacts as measured in this work. All quantities are given in units of eV, where e is the electron charge. eV_{bb} is the band bending in the Si.

The energy band diagram of this contact is presented in Fig. 5(a). We note that other values have been reported for BE_v(Si $2p_{3/2}$), including 98.80(5) eV [31] and 98.85(5) eV [32]. The value given by Himpsel et al. [30] (98.74(4) eV), used herein, gives the best agreement with prior reports of the n-Si(1 1 1)/Au Schottky barrier height. Using these other BE_v values would yield a slightly larger Schottky barrier height, by 50 or 110 meV, respectively.

3.2. Interface formation with Cu

3.2.1. Spectra at $E_{ex} = 330$ eV

Fig. 6 presents the survey spectra ($E_{ex} = 330$ eV) observed during the deposition of Cu on CH_3–Si(1 1 1). During Cu deposition, the substrate-related emissions (C 1s, Si LVV, Si 2s, Si 2p) decreased in intensity, whereas the Cu-related emissions (Cu MVV, Cu 3s, Cu 3p, Cu 3d) increased in intensity. The C 1s emission decreased in intensity, but did not completely disappear, as the Cu coverage increased. The Si 2p emission exhibited similar behavior. Additionally, after the last deposition step, the Si 2p peak broadened considerably and exhibited a chemical shift of ≈2–3 eV with respect to bulk silicon (Fig. 6).

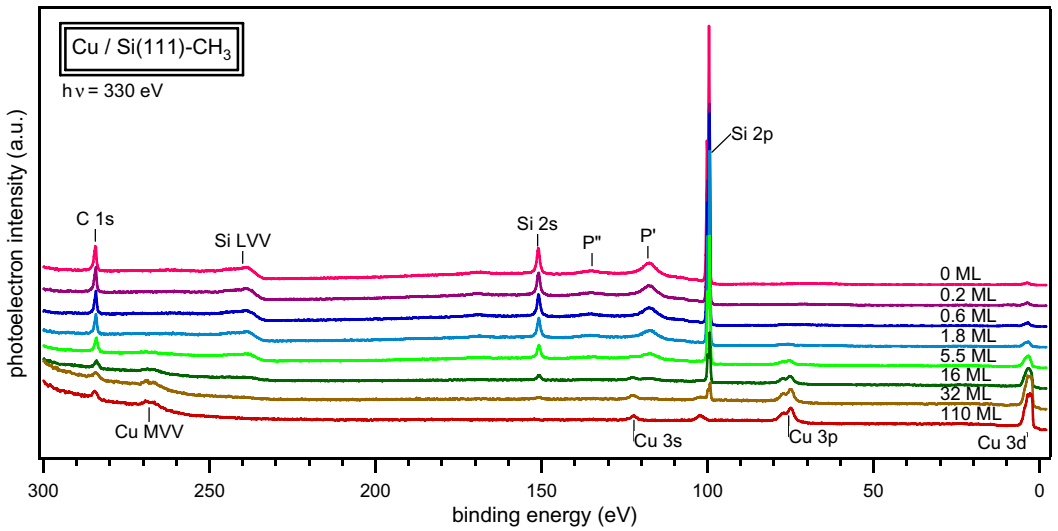

Fig. 6. Survey scans (with $E_{ex} = 330$ eV) of the stepwise deposition of Cu copper onto CH_3–Si(1 1 1). Apart from the photoelectron lines indicated, the Auger emissions Si LVV and Cu MVV were observed. Peaks labelled P′ and P″ correspond to plasmon loss lines of the Si 2p emission.

Fig. 7 displays the detailed SXPS data in the C 1s and Si 2p regions ($E_{ex} = 330$ eV). In the C 1s region, a shoulder at ≈283.4 eV, i.e. on the low binding energy side of the main peak, was observed for Cu coverages of 5, 16, or 32 ML. The shift of all of emission lines with increasing Cu coverage can be ascribed to the increasing band banding induced by the deposition of Cu.

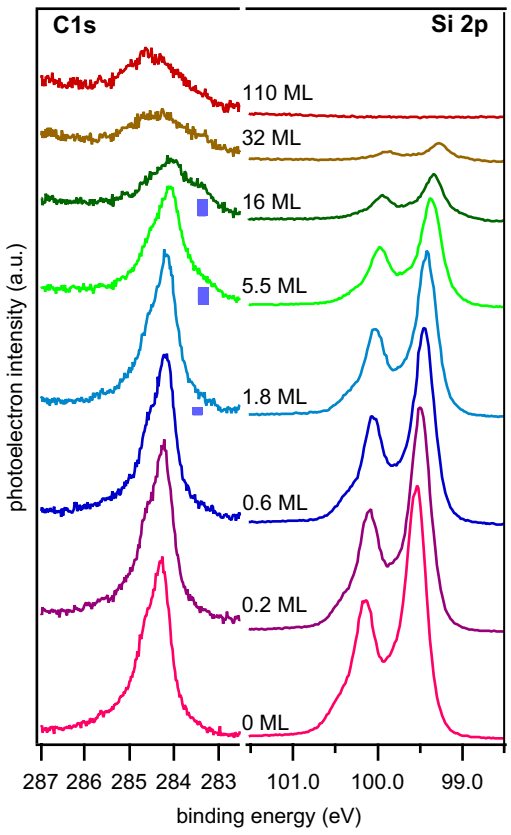

Fig. 7. C1s and Si 2p SXPS spectra as a function of the cumulative deposition of Cu onto CH_3–Si(1 1 1) ($E_{ex} = 330$ eV).

3.2.2. Si 2p spectra at $E_{ex} = 150$ eV

The more surface-sensitive Si 2p spectra obtained with $E_{ex} = 150$ eV are plotted in Fig. 8, together with fits of the spectral data. For clarity in presentation, the spectra were scaled as indicated to have similar maximum amplitudes.

For the first deposition steps, up to a Cu coverage of 0.6 ML, the Si 2p line shape remained essentially unchanged. In contrast, for nominal Cu coverages of 6 to 32 ML, a distinct shoulder was observed at low binding energy of the Si 2p emissions. The signal was barely observable for 2 ML of Cu coverage. The fits indicated that the low binding energy component had a chemical shift of −0.27(2) eV with respect to the bulk silicon emission, Si^0. A similar, chemically shifted lower binding energy component has been observed in previous synchrotron XPS studies [22,23]. In agreement with Refs. [21,22], this signal is assigned to the copper silicide $SiCu_3$ alloy. In an earlier report, the low BE component was, in contrast, assigned to a solid solution of silicon in copper [17].

Fig. 9 displays the evolution of the intensity of the different emission lines as the coverage of Cu increased. The highest intensity of the signal ascribed to the putative interfacial reaction product, $SiCu_3$, was observed for 5 ML Cu coverage, and corresponded to ≈1/5 of a ML of Si. With further deposition of Cu, the $SiCu_3$ component of the Si 2p signal was attenuated concomitantly with the bulk Si^0 component (Fig. 9). This behavior indicates that, in contrast to the situation for Au deposited on CH_3–Si(1 1 1), the $SiCu_3$ alloy did not float on top of the deposited Cu film, but was buried below an increasingly thick Cu layer.

The relative intensity of the (carbon-bound) Si 2p surface component, Si–CH_3, did not change as a result of either the onset of interface reaction or concomitant $SiCu_3$ formation. Instead, as long as the bulk silicon Si^0 emission was observed (⩽32 ML), the Si–CH_3-related emission was also observed without a significant change in relative intensity.

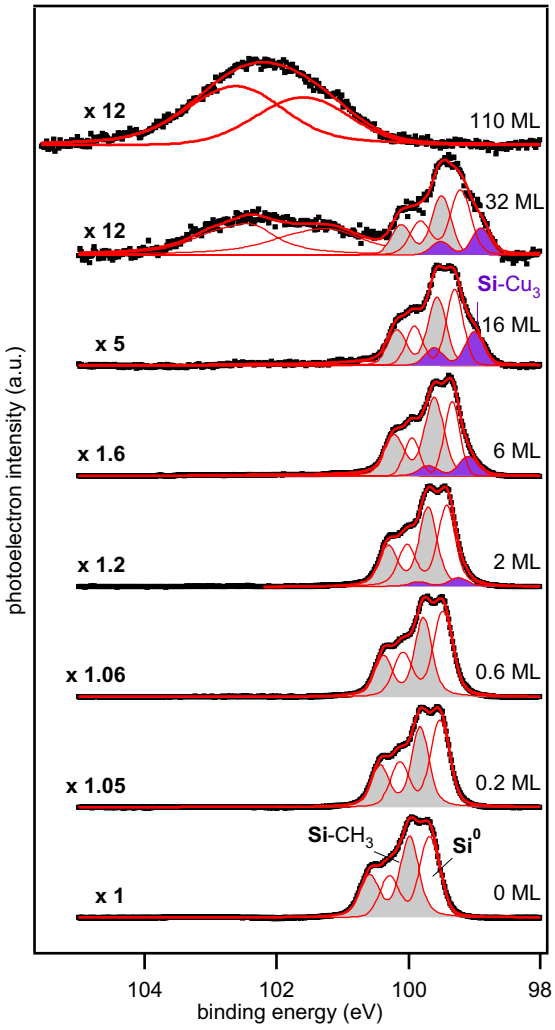

Fig. 8. Surface-sensitive Si 2p photoelectron spectra ($E_{ex} = 150$ eV) of the deposition of Cu onto CH_3–Si(1 1 1). The signal intensities have been scaled as labelled for ready viewing of the different spectra. The shaded peaks represent fits of the data to contributions from bulk Si^0, a CH_3-bound surface component (Si–CH_3), and copper silicide ($SiCu_3$) reacted Si species.

This behavior indicates that the methyl termination remained essentially intact between the Cu islands.

Fig. 9 also presents the intensity of the SXPS Si 2p signal as a result of the deposition of Cu on CH_3–Si(1 1 1). The attenuation of the silicon substrate emission up to a coverage of 16 ML (~4 nm) was well-described by an exponential decrease of the form $I = I_0 e^{-d/\lambda_{eff}}$, with an effective attenuation length, λ_{eff}, of 1.9 nm. This value is much larger than the inelastic mean free path (IMFP) of ≈0.4 nm for this electron kinetic energy [28]. This behavior implies that instead of a two-dimensional growth of the deposited Cu film, a three-dimensional growth occurred, with pronounced clustering of metal.

In addition to the observation of the $SiCu_3$ reaction product for a nominal coverage of $\geqslant 5.5$ ML, an increase was observed in the background on the high binding energy side of the Si 2p emission (Fig. 8). This signal developed

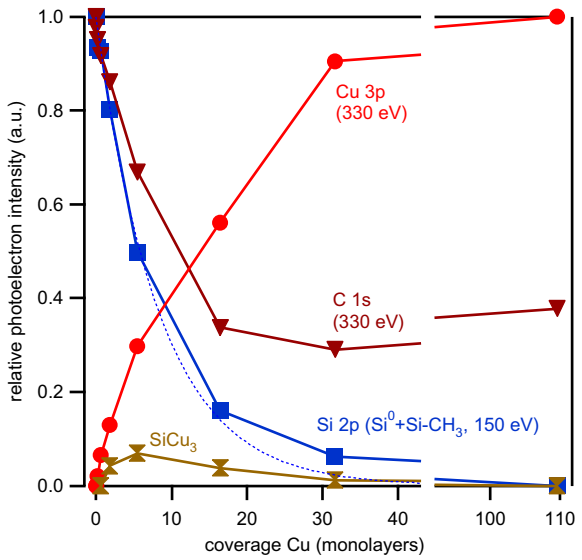

Fig. 9. Evolution of the photoelectron signal intensities as a function of Cu deposition onto CH_3–Si(1 1 1). The dotted line represents an exponential attenuation of the substrate Si 2p emission with an attenuation length of ~1.9 nm, which is far larger than the IMFP of 0.4 nm. The observed behavior is thus indicative of pronounced clustering. Upon disruption of the methyl termination and formation of $SiCu_3$ at >5 ML of Cu, the C 1s emission is less attenuated than the substrate silicon.

into a double-peak structure and displayed a considerable chemical shift with respect to Si^0. These components were best distinguished for 32 ML nominal coverage, with the Si 2p peaks at this point exhibiting chemical shifts of 2.0 eV and 3.0 eV, respectively with respect to bulk Si^0. These two Si 2p components were also observed for the highest nominal coverage, 110 ML, of Cu. The Cu film

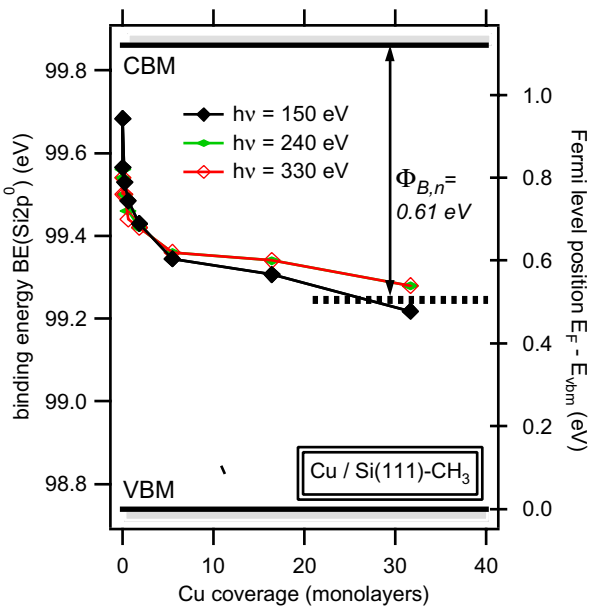

Fig. 10. Evolution of the band bending in the silicon as a function of the deposition of Cu onto the CH_3–Si(1 1 1) surface, as monitored by the binding energy shift of the Si $2p_{3/2}$ emission. A Schottky barrier height of 0.61(8) eV is obtained using $BE_v(Si^0\ 2p) = 98.74(4)$ eV.

was presumably closed at this coverage, and the remaining Si 2p emissions then would arise from silicon carbide and possibly from cuprous silicon carbide floating on top of the closed film of Cu metal.

3.2.3. Si 2p binding energy vs Cu coverage

The band bending during Cu deposition is evaluated quantitatively in Fig. 10, in which the energetics of the CH_3–Si(1 1 1)/Cu contact derived from the Si 2p binding energy are presented as a function of the Cu coverage. Using a value for the binding energy of Si 2p with respect to the valence band maximum of 98.74 eV [30], the distance of the Fermi-level from the valence band maximum, $E_F - E_v$, was calculated for each deposition step (right scale). From these data, an electronic Schottky barrier height, $\Phi_{B,n}$, of 0.61(8) eV was derived for the n-type CH_3–Si(1 1 1)/Cu Schottky contact. A surface band diagram of the n-type CH_3–Si(1 1 1)/Cu Schottky contact is given in Fig. 5(b).

4. Discussion

4.1. Reactivity of CH_3–Si(1 1 1) with Au

The clean Si(1 1 1) surface undergoes a (7×7) reconstruction to lower the surface free energy. Deposition of Au onto this reconstructed surface, to form a Schottky contact, has been shown to result in the formation of the metal silicide $SiAu_3$ [18,19]. For the Si(1 1 1)-(7×7) surface, formation of $SiAu_3$ has been observed for all levels of Au deposition [18]. The $SiAu_3$ surface layer increases in thickness until 3–4 ML have been produced. Upon further deposition of Au, the 3–4 ML thick $SiAu_3$ layer detaches from the Si substrate, and metallic Au accumulates beneath the $SiAu_3$ layer. Hence, an abrupt Si(1 1 1)/Au interface is generated, and the $SiAu_3$ forms a ''skin'' on top of the metallic Au film.

Chemical passivation of the Si(1 1 1) surface by hydrogen termination [20], or by use of a GaSe halfsheet termination, has been investigated to suppress the formation of the $SiAu_3$ film [24]. No significant difference in the final film structure, for high Au coverage, was observed between the Si(1 1 1)-(7×7) and Si(1 1 1):H surfaces, and a surface $SiAu_3$ skin of $\approx$2 ML in thickness was produced in each system [20]. In contrast, the formation of $SiAu_3$ is almost completely suppressed on the Si(1 1 1):GaSe surface. Nevertheless, substantial interfacial reactions occured on this surface, because $\approx$70% of the GaSe-termination layer appeared to be disconnected from the silicon surface, and segregated to the top of the growing Au layer [24].

For the CH_3–Si(1 1 1) surface, stoichiometric amounts of $SiAu_3$, i.e. a clearly distinguishable $SiAu_3$ component in the Si 2p region, were only observed for $\geqslant$0.5 ML of Au. This behavior indicates that methyl termination initially suppressed the interfacial reactivity of Si(1 1 1) with Au, but did not completely prevent the eventual formation of a $SiAu_3$ interfacial layer.

The observation of $\approx$1 ML of $SiAu_3$ from the Si 2p intensity data underscores that the silicide formed on CH_3–Si(1 1 1) is of $SiAu_3$ composition. The lack of change in the intensity or position of this signal with the further addition of Au indicated that the $SiAu_3$ phase was not buried at the Si/Au interface. Instead, with increasing Au coverage, the data indicate that the $SiAu_3$ layer migrated to the surface of the Au film and remained on top of the Au layer.

The behavior of the Si 2p and Au 4f emissions during deposition of Au indicated that the Si remained methyl-terminated in regions of the surface not covered with Au. The double-peak structure at the low binding energy side of the Si 2p emission, originating from bulk Si^0 and surface CH_3-bonded Si atoms, respectively, was clearly observed in the extremely surface-sensitive Si 2p spectra obtained using $E_{ex} = 150$ eV, at least up to a Au coverage of 6 ML. The inelastic mean free path of the Si 2p photoelectrons with a kinetic energy of 50 eV is as low as 0.4 nm [28], hence the Si 2p spectra obtained under such conditions effectively monitor only the outermost Si(1 1 1) bilayer, with the topmost monolayer consisting of Si bonded to $-CH_3$ groups. Thus, to a first approximation, under such conditions, the Au_3Si/Au clusters fully quench the emission from the underlying Si substrate. For this excitation energy, the relative intensity of the Si^0/Si–CH_3 emission compared to that of the bare substrate therefore indicates the fraction of the surface that is not covered by Au. The intensity ratio of methyl-bonded Si to bulk Si remained constant at about 0.84(5) for Au coverages $\leqslant$6 ML, consistent with the existence of methyl termination on areas that were not covered with Au. Clearly, the formation of the $SiAu_3$ surface phase, and its subsequent migration to the top of the Au layer, requires a disruption of the methyl termination and the concomitant out-diffusion of silicon atoms. The disruption of the methyl termination thus presumably occurred below the regions of deposited Au islands.

The observations indicate that the following ''reactivity scale'' can be formulated for Si(1 1 1) surfaces of various termination:

$$\begin{aligned}&\text{reactivity}[\text{Si}(1\,1\,1) - 7 \times 7/\text{Au}]\\ &\quad > \text{reactivity}[\text{CH}_3\text{–Si}(1\,1\,1)/\text{Au}]\\ &\quad > \text{reactivity}[\text{Si}(1\,1\,1)\text{–GaSe/Au}]\end{aligned}$$

This ''reactivity scale'' is derived from Fig. 11, in which the Si 2p and Au 4f emissions for similar Au coverage ($\approx$10 ML of Au) are compared for the CH_3–Si(1 1 1), GaSe halfsheet-terminated Si(1 1 1) [24], and bare 7×7-Si(1 1 1) interfaces with Au [24]. The $SiAu_3$-related Au 4f emissions are most intense for the bare 7×7-Si(1 1 1)/Au interface, somewhat smaller for the CH_3–Si(1 1 1)/Au interface, and least pronounced for the Si–GaSe/Au structure. The same trend is evident for the intensity of the Si 2p emission, in which the CH_3–Si(1 1 1)/Au interface does not display emissions at 101 eV and higher binding energies, which correspond to other reaction products. A quantitative analysis indicates that 3–4 ML of $SiAu_3$ are formed on

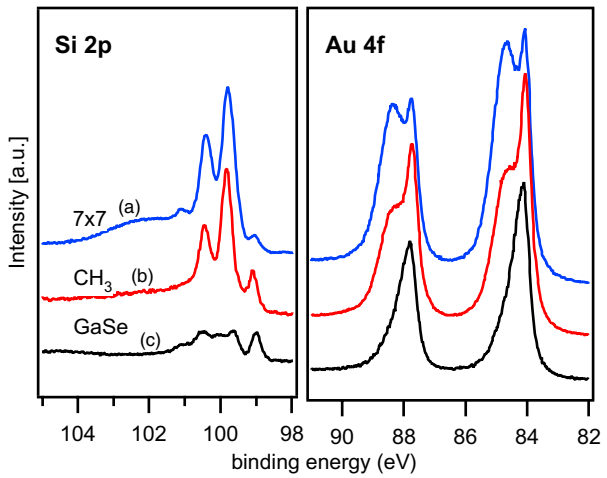

Fig. 11. Comparison of the Si 2p and Au 4f emissions ($E_{ex} = 240$ eV) for the Si(1 1 1)/Au Schottky contacts with surface termination consisting of: (a) (7×7) reconstruction (i.e. no termination layer); (b) methyl termination (CH_3); (c) GaSe halfsheet termination (GaSe). The data for the (7×7) and GaSe terminated surfaces are taken from Ref. [22]. The nominal Au film thickness is about 10 ML.

Si(1 1 1)-(7×7)/Au, ≈1 ML is formed on CH_3–Si(1 1 1)/Au, and only a small fraction of a monolayer is formed on Si(1 1 1)-GaSe/Au. For the Si–GaSe surface, the dissolution of surface silicon atoms is however replaced by the dissolution of the GaSe halfsheet termination.

The minimization of the surface free energy of the growing Au film appears to be the driving force for the observed interfacial reactions. A surface "skin" of a reacted Au compound is formed in all of the cases investigated, with $SiAu_3$ observed for the clean Si(1 1 1)-(7×7), the hydrogen-terminated Si(1 1 1):H, or the methylated CH_3–Si(1 1 1) surface, and with a Au–Ga–Se surface layer observed for the GaSe halfsheet termination of Si(1 1 1). The methyl termination is effective in that it reduces the amount of silicon consumed by the surface reaction from ≈1 ML of Si(1 1 1) in the case of Si(1 1 1)-(7×7)/Au contacts (surface atom density 8×10^{14} cm^{-2}) to ≈0.3 ML for Si(1 1 1)–CH_3/Au. The CH_3 termination, however, did not completely suppress the reactivity of the Si(1 1 1) surface.

4.2. Reactivity of CH_3–Si(1 1 1) with Cu

The reactivity of CH_3–Si(1 1 1) with Cu displayed some similarities, and some differences, with respect to the reactivity of CH_3–Si(1 1 1) with Au. Again the CH_3-termination prevented, but did not preclude, the eventual reaction of the surface with the deposited metal. The amount of interfacial reaction product formed, however, is far less on CH_3–Si(1 1 1) than on the non-methylated surface.

Upon deposition of ⩾2 ML copper, a chemically shifted, reacted Si 2p component was identified at binding energies of −0.27(2) eV from the Si^0 emission. This emission is assigned to $SiCu_3$ [21,22]. The evolution of the $SiCu_3$ component as a function of Cu coverage is similar for Si(1 1 1)-(7×7) surfaces [23] and the CH_3-terminated Si(1 1 1) surface investigated in this work. For both surfaces, the $SiCu_3$ signal reached a maximum for a coverage of about 6 ML, and was subsequently completely quenched (Fig. 9). In contrast to the behavior of the CH_3–Si(1 1 1)/Au interface, the $SiCu_3$ reaction product did not migrate to the top of the deposited Cu film, but remained buried at the interface as the Cu film thickness increased.

A major difference from the deposition on the bare (7×7) surface, however, lies in the amount of interfacial $SiCu_3$ formed. Fig. 12 presents the Si 2p emissions for similar Cu coverage (≈6 ML) for the methyl-terminated, GaSe halfsheet-terminated [32], and bare 7×7-Si(1 1 1)/Au interfaces, respectively [32]. The chemical components of reacted copper silicide ($SiCu_3$), bulk silicon (Si^0), and methyl-bound surface silicon (Si^+–CH_3) were evaluated by curve fitting and were also included in Fig. 12. For the room temperature deposition of Cu on non-passivated Si(1 1 1)-(7×7), the evolution of the spectral components was very similar to that in the literature [23]. For the (7×7) surface, the Si 2p signal from the interface is dominated by the $SiCu_3$ emission, which is shifted by −0.35 eV with respect to Si^0. The signal intensity is equivalent to several monolayers of $SiCu_3$. In contrast, for a comparable amount of Cu on CH_3–Si(1 1 1), the emission from $SiCu_3$ is much weaker, indicating that the methyl termination substantially suppressed the interfacial reaction. The maximum Si 2p[$SiCu_3$] intensity observed corresponded to the dissolution of about 0.2 ML of Si(1 1 1) ($N_{Si(111)} = 7.8 \times 10^{14}$ cm^{-2}).

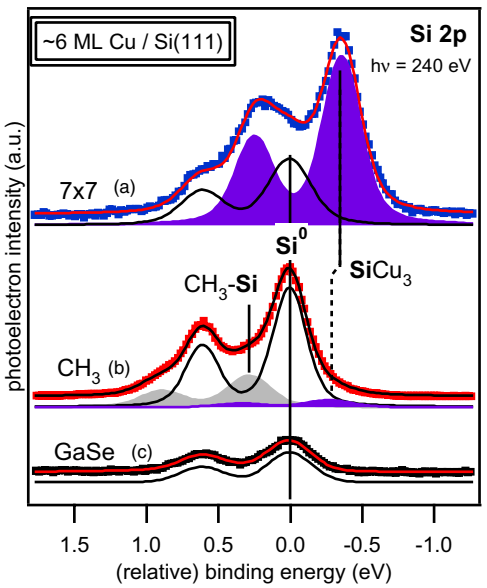

Fig. 12. Comparison of the Si 2p emissions ($E_{ex} = 240$ eV) for Si(1 1 1)/Cu Schottky contacts with surface termination consisting of: (a) (7×7) reconstruction (i.e. no termination layer); (b) methyl termination (CH_3); (c) GaSe halfsheet termination (GaSe). The data for the (7×7) and GaSe terminated surfaces are taken from Ref. [32]. The nominal Cu film thickness is ≈6 ML.

4.3. Schottky barrier heights

A motivation for investigation of the CH_3–Si(1 1 1)/Au and CH_3–Si(1 1 1)/Cu interfaces was the question of whether the surface dipole of −0.4 eV associated with the methyl termination [12] could be used to manipulate the energy level alignment at the semiconductor/metal junction. Table 3 presents a comparison of measured Schottky barrier heights of Si(1 1 1) with Au, for different terminations of the Si(1 1 1) surface. The measured electron barrier heights for GaSe halfsheet-terminated and methyl-terminated silicon were nominally identical, with a value of 0.78(8) eV. The differences from the reported values of the barrier heights of Au on Si(1 1 1)-(7 × 7) (0.81(4) eV) or Si(1 1 1):H (0.74(4) eV) surfaces [20] are within the experimental uncertainty.

In Table 4, the value for the Schottky barrier height of Cu on CH_3–Si(1 1 1) is compared to the reported barrier heights of Cu on Si(0 0 1), Si(1 1 1)-(7 × 7), and Si(1 1 1) terminated with a halfsheet of GaSe, respectively. As in the case of the Au contact, the Schottky barrier height of Cu on CH_3–Si(1 1 1), 0.61(8) eV, is close to the barrier height of Cu on the GaSe-terminated substrate, and the other Si surfaces. Again, any differences between the barrier heights of these surfaces are within the experimental uncertainty.

Thus, for both cases, Au or Cu deposition, the termination with –CH_3 groups partly suppressed reaction of the Si with metal, but eventually the resulting interface had very similar energetics to that obtained from deposition of Au or Cu onto the Si(1 1 1)-(7 × 7) surface.

Table 3
Electron Schottky barrier heights, $\Phi_{B,n}$, of Au contacts with n-Si(1 1 1)

System	$\Phi_{B,n}$ (eV)	Reference
n-Si(1 1 1)-(7 × 7)	0.81(4)	[20]
p^+-Si(1 1 1)-(7 × 7)	0.81(5)[a]	[24]
n-Si(1 1 1)–H	0.75(4)	[20]
n-Si(1 1 1)–GaSe	0.78(5)	[24]
n-Si(1 1 1)–CH_3	0.78(8)	This work

[a] The electron Schottky barrier, $\Phi_{B,n}$, was calculated from the measured hole Schottky barrier, $\Phi_{B,p}$, according to $\Phi_{B,p} + \Phi_{B,n} = E_g = 1.12$ eV. The constant $BE_v(Si^0\ 2p_{3/2}) = 98.74(4)$ from Ref. [30] was applied.

Table 4
Electron Schottky barrier heights, $\Phi_{B,n}$, of Cu contacts with Si

System	$\Phi_{B,n}$ (eV)	Reference
n-Si(0 0 1)	0.60[a]	[33]
n-Si(1 1 1)	0.62(1)[a]	[34]
p-Si(1 1 1)-(7 × 7)	0.67(5)[b]	[32]
p-Si(1 1 1)–GaSe	0.65(4)[b]	[32]
n-Si(1 1 1)–CH_3	0.61(8)	This work

[a] Determined from *I–V* (current–voltage) characteristics.

[b] The electron Schottky barrier, $\Phi_{B,n}$, was calculated from the measured hole Schottky barrier, $\Phi_{B,p}$, according to $\Phi_{B,p} + \Phi_{B,n} = E_g = 1.12$ eV. The constant $BE_v(Si^0\ 2p_{3/2}) = 98.74(4)$ from Ref. [30] was applied.

5. Conclusions

The formation of a Schottky junction by stepwise vacuum evaporation of Au or Cu onto methyl-terminated n-Si(1 1 1) was investigated by means of high-resolution SXPS. The methyl termination delayed, but ultimately did not prevent, reaction of the deposited metal with the Si surface for either gold or copper deposited under the conditions studied herein. Consistently, the appearance of chemically shifted silicon species, attributed to interfacial reactions reflecting the formation of the silicon–metal alloys $SiAu_3$ and $SiCu_3$, respectively, was observed by SXPS. As is the case for deposition of Au or Cu on the (7 × 7)-reconstructed Si(1 1 1) surface, the chemically shifted species on CH_3–Si(1 1 1) were observed at −0.74(2) eV, ($SiAu_3$) and +0.27(2) eV ($SiCu_3$) with respect to the bulk Si^0 emission. For both systems studied, however, the amount of metal silicide formed was substantially reduced relative to that formed on the Si(1 1 1)-(7 × 7) surface.

The electron Schottky barrier height, $\Phi_{B,n}$, was determined for the Au and Cu contacts to the methyl-terminated Si(1 1 1) surfaces. The measured barrier heights were 0.78(8) eV and 0.61(8) eV for CH_3–Si(1 1 1)/Au and CH_3–Si(1 1 1)/Cu interfaces, respectively. These values are within the experimental uncertainty identical to those observed when Au or Cu is deposited onto clean, reconstructed Si(1 1 1)-(7 × 7) surfaces. Thus, the electronic surface potential step of ≈−0.4 eV produced by methyl termination of the Si(1 1 1) surface [12] did not modify the energy level alignment of the metal relative to the silicon. This correlates with the observation that the methyl termination was partially destructed by the interface reaction that accompanied metal deposition under our conditions. To exploit the surface dipole of the methyl termination of Si(1 1 1) for the modification of interfacial transport barriers, non-reactive interfaces of silicon, using metals such as indium or silver, should be investigated.

Acknowledgements

We gratefully acknowledge the National Science Foundation, Grant CHE-0604894, for support of this work (N.S.L. and L.J.W.) and for providing a graduate research fellowship to L.J.W. W.J. acknowledges the travelling support of the Deutsche Forschungsgemeinschaft, DFG Grant No. JA 85910-1. The support of the BMBF for setting-up and running SoLiAS at BESSY (contracts 05 KS1RD1/0 and 05 KS4RD1/0, R.H. and W.J.) and travel Grants (05 ES3XBA/5) are gratefully acknowledged. This work was also supported by the European Network of Excellence FAME (WP 6).

References

[1] M.R. Linford, C.E.D. Chidsey, J. Am. Chem. Soc. 115 (1993) 12631.
[2] M.R. Linford, P. Fenter, P.M. Eisenberger, C.E.D. Chidsey, J. Am. Chem. Soc. 117 (1995) 3145.

[3] A.B. Sieval, A.L. Demirel, J.W.M. Nissink, M.R. Linford, J.H.v.d. Maas, W.H.d. Jeu, H. Zuilhof, E.J.R. Sudhölter, Langmuir 14 (1998) 1759.
[4] R.L. Cicero, M.R. Linford, C.E.D. Chidsey, Langmuir 16 (2000) 5688.
[5] A. Bansal, X. Li, I. Lauermann, N.S. Lewis, S.I. Yi, W.H. Weinberg, J. Am. Chem. Soc. 118 (1996) 7225.
[6] A. Bansal, X. Li, S.I. Yi, W.H. Weinberg, N.S. Lewis, J. Phys. Chem. B 105 (2001) 10266.
[7] D. Niwa, T. Inoue, H. Fukunaga, T. Akasaka, T. Yamada, T. Homma, T. Osaka, Chem. Lett. 33 (2003) 284.
[8] L.J. Webb, N.S. Lewis, J. Phys. Chem. B 107 (2003) 5404.
[9] T. Yamada, M. Kawai, A. Wawro, S. Suto, A. Kasuya, J. Chem. Phys. 121 (2004) 10660.
[10] L.J. Webb, E.J. Nemanick, J.S. Biteen, D.W. Knapp, D.J. Michalak, M.C. Traub, A.S.Y. Chan, B.S. Brunschwig, N.S. Lewis, J. Phys. Chem. B 109 (2005) 3930.
[11] H. Yu, L.J. Webb, R.S. Ries, S.D. Solares, W.A. Goddard III, J.R. Heath, N.S. Lewis, J. Phys. Chem. B (2005) 671.
[12] R. Hunger, R. Fritsche, B. Jaeckel, W. Jaegermann, L.J. Webb, N.S. Lewis, Phys. Rev. B 72 (2005) 045317.
[13] E.J. Nemanick, S.D. Solares, W.A. Goddard, N.S. Lewis, J. Phys. Chem. B 110 (2006) 14842.
[14] E.J. Nemanick, P.T. Hurley, B.S. Brunschwig, N.S. Lewis, J. Phys. Chem. B 110 (2006) 14800.
[15] W.J. Royea, A. Juang, N.S. Lewis, Appl. Phys. Lett. 77 (2000) 1988.
[16] M. Hanbucken, Z. Imam, J.J. Metois, G. Le Lay, Surf. Sci. 162 (1985) 628.
[17] M. del Giudice, J.J. Joyce, J.H. Weaver, Phys. Rev. B 36 (1987) 4761.
[18] J.J. Yeh, J. Hwang, K. Bertness, D.J. Friedman, R. Cao, I. Lindau, Phys. Rev. Lett. 70 (1993) 3768.
[19] S.L. Molodtsov, C. Laubschat, G. Kaindl, A.M. Shikin, V.K. Adamchuk, Phys. Rev. B 44 (1991) 8850.
[20] C. Grupp, A. Taleb-Ibrahimi, Phys. Rev. B 57 (1998) 6258.
[21] G. Rossi, I. Lindau, Phys. Rev. B 28 (1983) 3597 LP.
[22] M. De Santis, M. Muntwiler, J. Osterwalder, G. Rossi, F. Sirotti, A. Stuck, L. Schlapbach, Surf. Sci. 477 (2001) 179.
[23] K. Pedersen, T.B. Kristensen, T.G. Pederser, P. Morgen, Z. Li, S.V. Hoffman, Phys. Rev. B 66 (2002) 153406.
[24] R. Fritsche, B. Jaeckel, A. Klein, W. Jaegermann, Appl. Surf. Sci. 234 (2004) 321.
[25] T. Mayer, M.V. Lebedev, R. Hunger, W. Jaegermann, Appl. Surf. Sci. 252 (2005) 31.
[26] M.P. Seah, W.A. Dench, Surf. Intf. Anal. 1 (1979) 2.
[27] J. Terry, M.R. Linford, C. Wigren, R. Cao, P. Pianetta, C.E.D. Chidsey, J. Appl. Phys. 85 (1999) 213.
[28] S. Tanuma, C.J. Powell, D.R. Penn, Surf. Interface. Anal. 17 (1991) 911.
[29] A.F. Lee, D.E. Gawthrope, N.J. Hart, K. Wilson, Surf. Sci. 548 (2004) 200.
[30] F.J. Himpsel, G. Hollinger, R.A. Pollak, Phys. Rev. B 28 (1983) 7014.
[31] A. Goldmann, E.-E. Koch, in: T.C. Chiang, F.J. Himpsel (Eds.), Landolt-Börnstein, New Series, vol. III, Springer, Heidelberg, 1989, p. 1.
[32] R. Fritsche, Dissertation, TU Darmstadt, 2004.
[33] M.O. Aboelfotoh, A. Cros, B.G. Svensson, K.N. Tu, Phys. Rev. B 41 (1990) 9819.
[34] A. Thanailakis, Journal of Physics C: Solid State Physics 8 (1975) 655.